Study on an active correction algorithm of primary mirror

Xiaolin Dai[1,2,3], Hao Xian[1,2], Xuejun Zhang[1,2] and Yudong Zhang[1,2]

[1]The key laboratory of adaptive optics, Chinese Academy of Sciences, 1 Xiahanggang Ave. Chengdu, China

[2]Institute of Optics and Electronics, Chinese Academy of Sciences, 1 Xihanggang Ave. Chengdu, China

[3]University of Chinese Academy of Sciences, Beijing, China

Abstract. The effects of active correction for the telescopes' primary mirrors are often degraded because the axial fixed points of the primary mirrors usually aren't able to perform active correction. This paper analyzes this problem and proposes a modified active correction algorithm to eliminate the adverse influence of the axial fixed points. We use a 1.2m thin mirror to simulate the modified algorithm, it shows the modified algorithm can significantly eliminate the adverse influence of the fixed points and improve the mirror's active correction effect: the fitting error of the 1.2m thin mirror on the 5th Zernike aberration reduces from 13nm to 1.6nm, the fitting errors for other Zernike aberrations also significantly reduce.

1. Introduction

Active optics is one of the key technologies to build large modern telescopes. By detecting the wavefront and correcting the mirror surface correspondingly, active optics can reduce the influence of the mirror's deformations on the beam quality and improve the observation capability of the large telescopes[1,2].

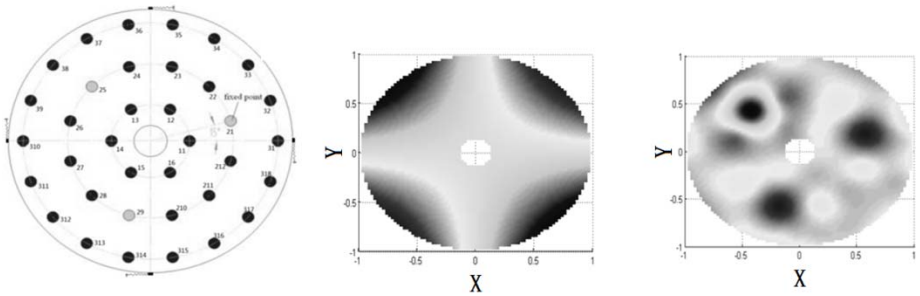

Figure. 1: (A): configuration of axial supports for an 1.2m thin mirror;
(B): 1.2 mirror's surface before active correction, a 5th Zernike aberration is taken for example;
(C): 1.2m mirror's surface after active correcting the deformations in (B).

Thin mirrors are widely used in large modern telescopes. Figure. 1(A) shows a typical axial supports' configuration of a thin mirror, there are 3 axial fixed points on the back of the mirror which are used to locate the primary mirror. These points can't generate axial motion or apply active correction forces, which causes an issue: mirror surface around these points can't be actively corrected thus degrading the active correction effect of the mirror(Figure. 1(B) and Figure. 1(C)). Floatation support is the most frequently adopted method to solve this problem[3-8], it consists of two steps:

firstly, measures the deformations of the mirror, calculates the correction forces(CF) and corrects the surface of the mirror; secondly, after the correction in the first step, measures the forces supported by the fixed points and modifies CF in term of eliminating the unbalanced moment on the mirror caused by the fixed points' forces. The second step is called the second step correction. But this method also has some issues: on one hand, a primary mirror which adopts floatation support has to apply the forces to the actuators for two times during each active correction process, which increases the time cost and leads to the decrease of correction frequency; on the other hand, the range of the correction forces in the first step is usually larger than the one after the second step(which is the range of the final correction forces), this increases the motion requirement of the actuators.

This paper firstly introduces the active correction's process and analyzes the adverse influence of the axial fixed points on the mirror surface's active correction in section 2. In section 3 we proposes a modified algorithm, this new algorithm can eliminate the axial fixed points' influence without introducing the second step correction. In section 4, we verifies the new algorithm via a simulation. The result shows the new algorithm is significantly effective: compared with the unmodified algorithm, the residual mirror surface RMS after the modified algorithm is greatly reduced.

2. Principle of the Active Correction

2.1 Principle of the Active Correction

Figure. 2 shows the principle of the active correction, it consists of 3 steps:

(1) Calibrate the actuators' interacting functions to the primary mirror surface. Firstly, measure W_0 by shooting the reference wave front W_{ref} to the mirror. Secondly, apply unit force to each actuator to make the mirror deform from M_1(ideal parabolic surface) to $M_{1(1)}$, $M_{1(2)}$, $M_{1(3)}$, … $M_{1(m)}$, then measure the corresponding wave fronts W_i(i=1,2,3…m). Lastly, because of the beam reflection at the mirror surface, the interacting function of each actuator to the mirror surface is $P_i = (W_i - W_0)/2$, (i=1,2,3…m).

(2) Measure the deformations of the primary mirror. Firstly, measure and reconstruct the wavefront W_{origin} at the exit pupil of the telescope, as Zernike modes are the most widely used bases in active correction, W_{origin} can be decomposed into Zernike modes here. Secondly, eliminate the first three Zernike modes from W_{origin} to get W. Thus the mirror's surface before active correction can be calculated as $W_{mirror} = W/2 = \sum_{i=4}^{n} a_i Z_i$, where Z_i is Zernike mode and a_i is the coefficient.

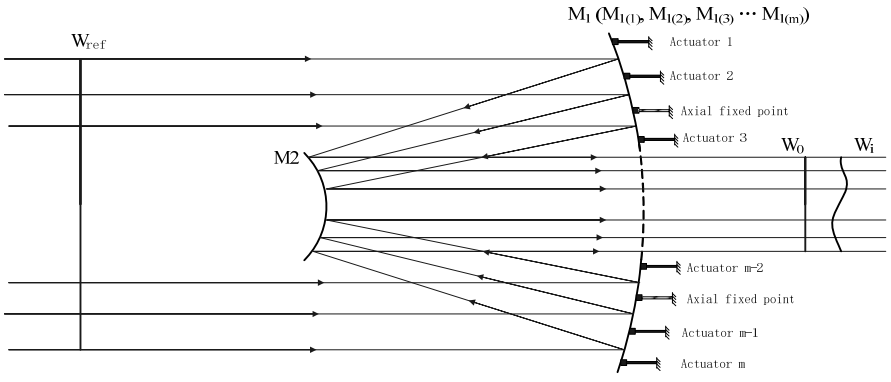

Figure. 2: Schematic of the Active Correction Algorithm.

(3) Calculate the correction force matrix of the actuators via the least square estimation. Assume the interacting function of each actuator measured in step (1) is P_i(i=1,2,3…m), the interacting function matrix will be $P=[P_1, P_2, \dots P_m]$, assume the correction force matrix of the actuators is $F=[F_1, F_2, \dots F_m]^T$, we have:

$$-W_{mirror} = -\sum_{i=4}^{n} a_i Z_i = P \cdot F \tag{1}$$

F can be calculated via the least square estimation as follows:

$$F = (P^T \cdot P)^{-1} \cdot P^T \cdot -W_{mirror} = (P^T \cdot P)^{-1} \cdot P^T \cdot -\sum_{i=4}^{n} a_i Z_i \tag{2}$$

By applying F to the actuators, the mirror deformations and the wavefront distortion at the exit pupil of the telescope could be corrected, which also means the surface of the primary mirror is corrected to the ideal parabolic M_1. Circulate steps (2) and (3) during the operation of the telescope and the mirror surface can be corrected in real time.

2.2 The Defection caused by the fixed points

During the implementation of the active correction, when the mirror deformations W_{mirror} is obtained, the algorithm usually will go to step (3) to calculate the correction force matrix F, but this leads to a problem. Shown in Figure. 3, curve 1 is the ideal parabolic mirror surface M_1 while curve 2 is W_{mirror}, if now we use the actuators to directly correct W_{mirror} to M_1, because the fixed points can't generate active motion, the final surface after active correction will be curve 3.

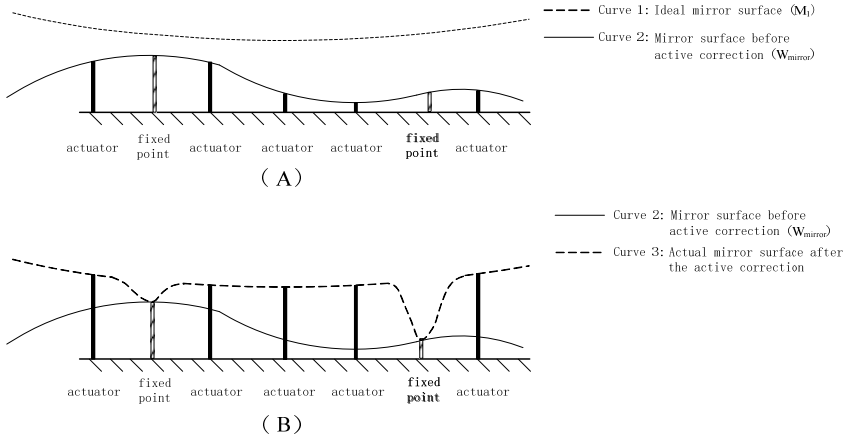

Figure. 3: the effect when using the actuators to directly correct W_{mirror} (profile map).

Figure. 3 shows that the mirror's active correction capability at the fixed points is limited, as a result the mirror surface after active correction is not an ideal parabolic but a curve with some "dents" at the fixed points, which degrades the effect of the active correction.

3. Modified Active Correction Algorithm

To reduce the adverse influence of the fixed points, a modified algorithm is proposed. This new algorithm firstly modifies the ideal parabolic surface M_1 to M_1', then calculates the correction force matrix according to W_{mirror} and M_1'. The core idea of the modification is: by adding M_1 a piston and one or two tilts to get M_1' which overlaps with W_{mirror} at the fixed points. Below is the detailed instruction of this algorithm.

Figure. 4(A) shows the modification of a 2-dimension M_1, assume the coordinates of the two fixed points are x_1,x_2 and the deviations of W_{mirror} from M_1 are s_1,s_2 (Figure. 4(A) is a profile map of a primary mirror, where M_1 and W_{mirror} are 2-dimension curves). Assume a modification curve $M_{correct}$ whose function is $y=a+lx$, $M_{correct}$ means a piston and a tilt, we have:

$$a + l\begin{bmatrix} x_1 \\ x_2 \end{bmatrix} = -\begin{bmatrix} s_1 \\ s_2 \end{bmatrix} \tag{3}$$

Equation (3) means: by adding a modification curve $M_{correct}$, the modified curve M_1'(=M_1+$M_{correct}$) will overlap with W_{mirror} at the fixed points(shown in Figure. 4, curve 3).

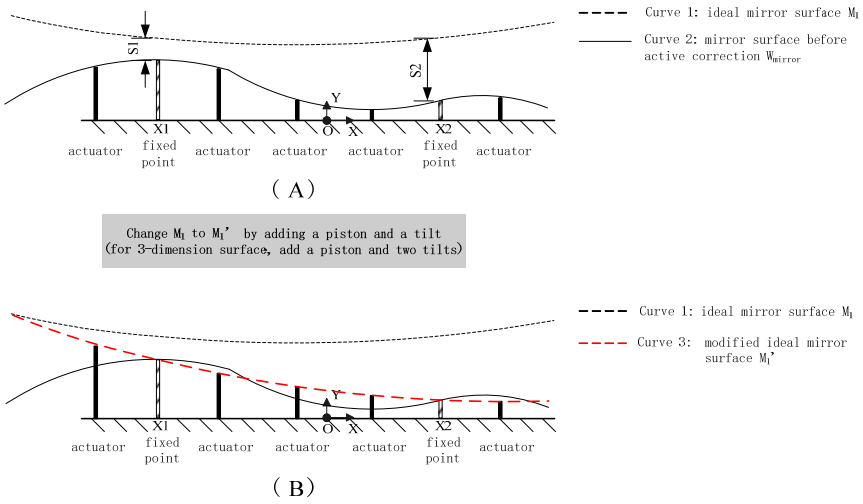

Figure. 4: Process of the modification of M_1.

After obtaining a and l via Equation. (3), we have:

$$M_1' = M_{correct} + M_1 \tag{4}$$

Figure. 4(B) shows the modified ideal mirror surface M_1' satisfies $M_1'(x=x_1) = W_{mirror}(x=x_1)$, $M_1'(x=x_2) = W_{mirror}(x=x_2)$, which means M_1' overlaps with W_{mirror} at the fixed points. To correct W_{mirror} to M_1', because the deviations of W_{mirror} from M_1' at $x=x_1$ and $x=x_2$ are 0 now, the fixed points actually don't need to generate any shift or motion during the correction, thus the adverse influence of the fixed points is eliminated. The mirror surface after active correction will be precisely M_1'.

Notice that M_1' is not the ideal surface M_1, the differences between them are a piston(a) and a tilt(l), these are actually some new distortions introduced into the telescope system, but they can be corrected by the telescope(for example by the secondary mirror) easily at the same time with the primary mirror's active correction process, so at last, we can virtually obtain the ideal parabolic surface M_1.

The reason why we don't adopt the second and third Zernike modes which are eliminated in step (2), section 2.1 as the tilts l_x and l_y which we need in the modification is that these two Zernike distortions can be caused by both the primary mirror and the second mirror, and the two parts can't be separated, thus they are different from l_x, l_y and can't be utilized directly here.

4. Simulation of the Modified Active Correction Algorithm

A 1.2m thin primary mirror is used to simulate the modified algorithm. Figure. 1(A) shows the configuration of the axial supports of the mirror, the diameters of the mirror and its central hole are 1.2m and 0.14m, the thickness is 50mm, radius-thickness ratio is 24. The material of the mirror is glass ceramics. There are 36 axial supports on the back of the mirror, the 21th, 25th and 29th supports are axial fixed supports or fixed points, which uniformly distribute on the 2th support ring, the rest 33 supports are active supports(actuators) which can apply active forces to the mirror. On the lateral side of the mirror there are 12 uniformly distributed lateral supports which can apply tangential support forces. In addition, there are 4 lateral fixed supports on the top, bottom, left and right of the mirror, which limit the 6 degrees of freedom of the mirror together with the 3 axial fixed points.

The active correction of the 5th Zernike aberration(astigmatism) via the 1.2m mirror is taken as an example to verify the effect of the modified algorithm. The simulation is implemented as follows:

(1) Calibrate the 33 actuators' interacting functions to the mirror surface and record them as P_i(i=11,12,13…22,23…317,318), part of the interacting functions are shown in Figure. 5.

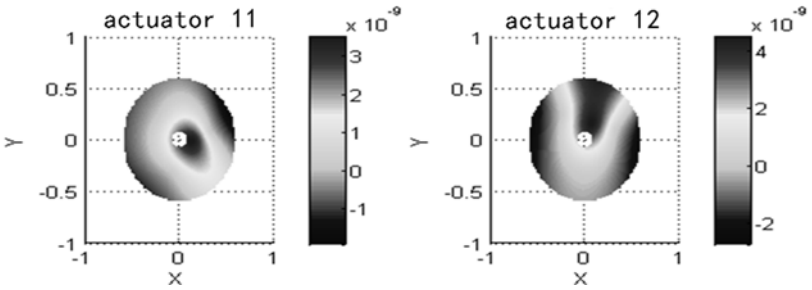

Figure. 5: part of the interacting functions of the active supports.

(2) Measure the deformations of the mirror. The amplitude of M_1 on Z axis is assumed to be 0. The mirror surface before active correction is shown in Figure. 6(left) as W_{mirror} (the radius has been normalized) whose RMS is about 100nm. Figure. 6(left) shows that the deviations of W_{mirror} from M_1 at the 3 fixed points are not zero, which means M_1 doesn't overlap with W_{mirror} at the fixed points. If now we correct W_{mirror} directly without any modification, the surface after the correction is shown in Figure. 6(right), the residual deviation has obvious peaks and valleys at the axial fixed points, the RMS of the residual deviation is about 13nm. Meanwhile, the correction forces of the actuators are shown in Figure. 7(blue line), the range of the forces is about -27N~40N.

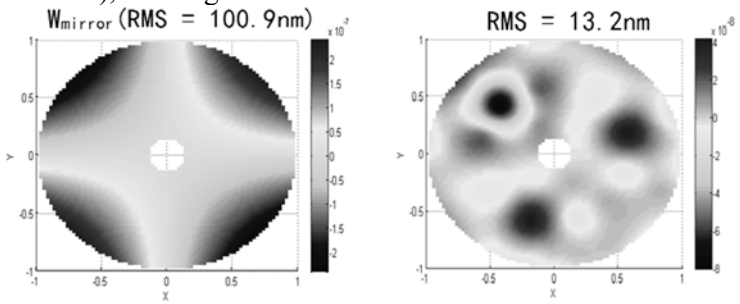

Figure. 6: left: mirror surface before active correction;
right: mirror surface after directly correction of W_{mirror}.

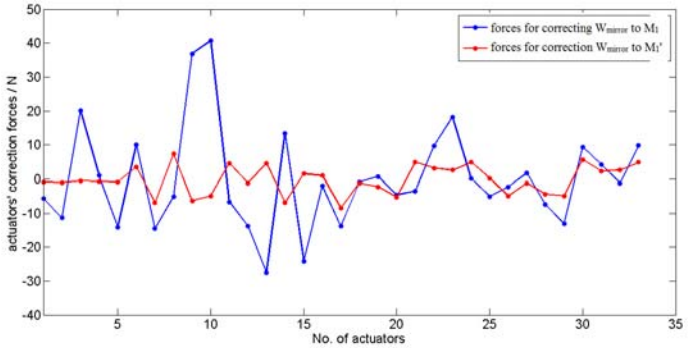

Figure. 7: correction forces of the 1.2m mirror's actuators for correcting W_{mirror} to M_1(blue line) and W_{mirror} to M_1' (red line). The 33 actuators on X axis corresponds sequentially to the actuators 11,12,13…16,22,23…212,31,32…318 in Figure. 1(A).

(3) Modify M_1. Firstly, the coordinates of the 3 fixed points on X-Y plain are calculated out: (0.5586m,0.1497m), (-0.4089m,0.4089m), (-0.1497m,-0.5586m), the deviations from W_{mirror} to M_1 at these 3 points are 33.7nm, -83.3nm, 42.3nm. Secondly, assume a modification curve $M_{correct}$ whose function is $z=a+l_x x+l_y y$ ($M_{correct}$ means a piston aberration and two tilt aberrations, where z axis overlaps with the optical axis of the primary mirror), we have the following equations:

$$a+\begin{bmatrix} 0.5586 & 0.1497 \\ -0.4089 & 0.4089 \\ -0.1497 & -0.5586 \end{bmatrix}\begin{bmatrix} l_x \\ l_y \end{bmatrix}=-\begin{bmatrix} 3.37\times10^{-8} \\ -8.33\times10^{-8} \\ 4.23\times10^{-8} \end{bmatrix} \quad (5)$$

Solve the equations above and we can obtain $M_{correct}$:

$$a = 2.45e-9 \quad l_x = -1.05e-7 \quad l_y = 9.28e-8 \tag{6}$$

Thus M_1' can be obtained via Equation (4). After the modification, the deviations of W_{mirror} from M_1' at the 3 fixed points are nearly zero.

(4) Calculate the correction forces for correcting W_{mirror} to M_1' via the least square estimation. The interacting function matrix of the actuator alignment is P=[P_{11} P_{12} … P_{317} P_{318}], assume the correction forces matrix to be F, then F could be computed via Eq. (7). At last, apply F to the actuators and at the same time use the second mirror to correct the extra piston a and tilts(l_x, l_y) to accomplish the active correction of the primary mirror.

$$F = (P^T \cdot P)^{-1} \cdot P^T \cdot (M_1' - W_{mirror}) \tag{7}$$

Figure. 7(red line) shows the values of *F*, the range of the forces is about -8.5N~7.3N, which significantly decreases compared with the range of the blue line.

The residual deviation of the 1.2m mirror surface after the correction via the new algorithm is shown in Figure. 8, contrasted with Figure. 6(right), the residual deviation of the mirror surface is significantly reduced, the peaks and valleys at the 3 fixed points basically disappear, the RMS of the residual deviation is reduced from 13nm to 1.6nm.

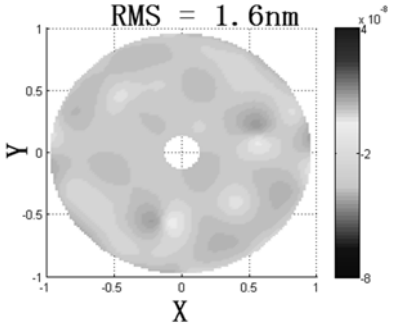

Figure. 8: the residual deformations of the 1.2m mirror surface after the correction with modified algorithm.

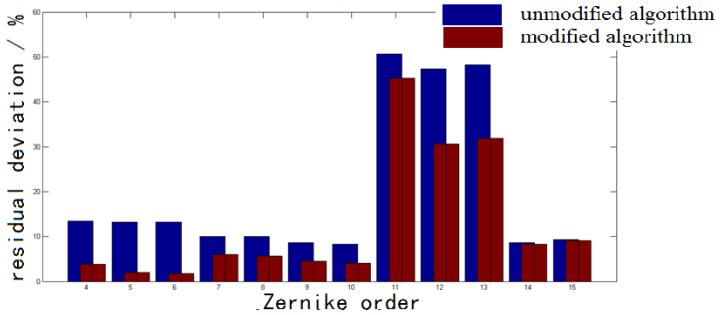

Figure. 9: the effects of the correction of the 1.2m thin mirror on different Zernike aberrations with unmodified and modified algorithm.

The effect of the modified correction algorithm on correcting the 4th~15th Zernike aberration via the 1.2m mirror is also simulated. Set the original mirror deformation to about 100nm, the effects of the active correction of the mirror with unmodified and modified algorithm are shown in Figure. 9, where the residual deviation is the ratio of mirror surface RMS after and before active correction. Figure. 9 shows that contrasted with the unmodified algorithm, the residual deviation of most Zernike aberrations after the correction improve significantly when adopting the modified algorithm. In addition, the range of the correction forces also decreases.

5. Conclusion

This paper firstly introduces the principle of active correction and analyzes one of its problem - the axial fixed points may degrade the primary mirror surface's active correction effect because they can't perform active axial motion; Secondly proposes a modified active correction algorithm which can eliminate the adverse influence of the fixed points; Lastly applies the algorithm to a 1.2m thin mirror to verify the new algorithm. The simulation shows that this new algorithm can effectively eliminate the influence of the fixed points, the RMS of the residual deviations of the mirror surface decreases significantly.

References

[1] L. Noethe. 2002. Active Optics in Modern, Large Optical Telescopes. *Progress in Optics*, vol. **43**, 3-69.
[2] Cheng Jingquan. 2003. Principles of Astronomical Telescope Design. Chinese Science & Technology Press, Beijing.
[3] B. C. H. M. Martin, L. R. Dettmann. 2004. Active optics and force optimization for the first 8.4 m LBT mirror. *Proc. SPIE* **5489**, 826-837.
[4] S. P. C. H. M. Martina, B. Cuerdena. 1998. Active supports and force optimization for the MMT primary mirror. *Proc. SPIE* **3352**, 412-423.
[5] D. G. James E. Kimbrell. 1998. AEOS 3.67 m Telescope Primary Mirror Active Control System. *Proc. SPIE* **3352**, 400-411.
[6] X. C. M. Schneerrnann, D. Enard. 1990. ESO VLT III : the support system of the primary mirror. *Proc. SPIE* **1236**, 920-928.
[7] E. D. Thomas A. Sebring, Robert L. Millis. 2004. The Discovery Channel Telescope A Wide Field Telescope in Northern Arizona. *Proc. SPIE* **5489**, 658-666.
[8] Li Hongzhuang, Zhang Zhenduo, Wang Jianli. 2013. Active Surface-Profile Correction of 620mm Thin-Mirror Based on Flotation Support. *Acta optica sinica*, vol. **33**, 0511001.